Articles

Novel Sol−Gel Synthesis of Sodium Aluminophosphate Glass Based on Aluminum Lactate

Long Zhang, Jerry C. C. Chan, and Hellmut Eckert*

Institut für Physikalische Chemie, Westfälische Wilhelms-Universität Münster, Schlossplatz 7, D-48149 Münster, Germany

Gundula Helsch, Lars P. Hoyer, and Günther H. Frischat*

Institut für Nichtmetallische Werkstoffe, Technische Universität Clausthal, Zehntnerstrasse 2a, D-38678 Clausthal-Zellerfeld, Germany

Received January 15, 2003. Revised Manuscript Received April 29, 2003

A novel sol−gel route based on aluminum lactate and sodium polyphosphate aqueous solutions has been developed to produce sodium aluminophosphate gels and glasses with the composition 43.8:12.5:43.8 $Na_2O/Al_2O_3/P_2O_5$. Preparations were optimized on the basis of detailed ^{27}Al solution- state NMR data, revealing the nature of the dominant precursor species as a function of pH and gelation temperature. A pH range of 1.8 to 3.6 was found to provide optimum conditions for the formation of homogeneous and transparent glasses. This pH range corresponds to the maximum concentration of mixed $Al(lact)_1(H_2O)_4^{2+}$ and the $Al(lact)_2(H_2O)_2^{+}$ precursor complexes, which appear to have the highest reactivity toward phosphate. The further replacement of lactate by phosphate ligands is favored by increasing the gelation temperatures above ambient. Upon heating to 400 °C the gels are converted to bulk glasses with thermal and structural characteristics identical to those of glasses prepared via traditional melt-cooling from 1350 °C. Solid-state ^{27}Al and ^{31}P NMR data and $^{27}Al\{^{31}P\}$ rotational echo double resonance (REDOR) spectra in particular confirm that the degree of Al/P connectivity is virtually identical in the glassy materials prepared by both routes. Thin films of this material have been prepared successfully on silica substrates and subsequently characterized by atomic force microscopy (AFM) and secondary neutral mass spectrometry (SNMS). These data indicate that the amount of residual carbon can be removed oxidatively upon heating by using $HClO_4$ rather than HCl as the proton source.

Introduction

The sol−gel process has become a quite attractive technique for the preparation of oxide glasses with a great variety of chemical compositions. The low processing temperatures offer unique opportunities for compositional and structural tailoring, while mixing of the starting materials on the molecular scale carries the prospect of making bulk samples and thin films with a high degree of chemical homogeneity.[1] Although much of the initial work in this area focused on the preparation of silicate-based materials, more recently the development of sol−gel routes toward non-siliceous glasses has attracted considerable interest. For example, extensive work during the past decade has been devoted to the processing and characterization of sol−gel derived aluminophosphate materials,[2−7] which have promising applications in hermetic seals,[8] as catalysts or catalyst supports,[2,4] and in laser and nonlinear optical devices.[9] The introduction of alumina into multiple-network former systems has remained a considerable challenge, because commonly used aluminum alkoxide precursors are highly reactive toward water, resulting in rapid hydrolysis and precipitation processes.[10] Approaches

* Authors to whom correspondence should be addressed. H.E.: Phone 49-251-832-9161; Fax 49-251-832-9159; E-mail eckerth@uni-muenster.de. G.H.F.: Phone 49-5323-72-2463; E-mail guenther.frischat@tu-clausthal.de.

(1) (a) Woigner, T.; Phallippou, J.; Zarzycki, J. *J. Non-Cryst. Solids* **1984**, *63*, 117. (b) Brinker, C. J.; Scherer, G. W. *Sol−Gel Science: The Physics and Chemistry of Sol−Gel Processing*; Academic Press: San Diego, CA, 1990. (c) Hench, L. L.; West, J. K. *Chem. Rev.* **1990**, *90*, 33.

(2) Glemza, R.; Parent, Y. O.; Welsh, W. A. *Catal. Today* **1992**, *14*, 185.

(3) Prabakar, S.; Rao, K. J.; Rao, C. N. R. *Mater. Res. Bull.* **1991**, *26*, 805.

(4) (a) Harmer, M. A.; Vega, A. J.; Flippen, R. B. *Chem. Mater.* **1994**, *6*, 1903. (b) Harmer, M. A.; Vega, A. J. *Solid State Nucl. Magn. Reson.* **1995**, *5*, 35. (c) Prabakar, S.; Rao, K. J.; Rao, C. N. R. *Mater. Res. Bull.* **1991**, *26*, 805.

(5) Lugmair, C. G.; Tilley, T. D.; Rheingold, A. L. *Chem. Mater.* **1999**, *11*, 1615.

(6) Montagne, L.; Palavit, G. *J. Non-Cryst. Solids* **1993**, *155*, 115.

(7) Lima, E. C. O.; Falembeck, G. J. *Colloid Interface Sci.* **1994**, *166*, 309.

(8) Brow, R. K.; Kovacic, L.; Loehman, R. E. *Ceram. Trans.* **1996**, *70*, 177.

(9) Weber, M. J. *J. Non-Cryst. Solids* **1990**, *123*, 208.

10.1021/cm030155g CCC: $25.00
Published on Web 06/10/2003

combatting this problem include (a) addition of the alumina source to prehydrolyzed sols containing the other constituents,[11] or (b) reducing the basicity of the aluminum precursors by choice of suitable ligands and complexation reagents.[12] For example, some new sol−gel routes based on aluminum-tri-*sec*-butoxide ($Al(OBu^s)_3$), modified with ethylacetoacetate, oxalic acid, ethanolamine, butane diol, etc., were successfully developed to prepare aluminum phosphate and other one- or two-component alumina-based materials (e.g., alumina and magnesia-alumina).[4,11−15] Despite these possibilities, the sol−gel chemistry of the ternary $Na_2O-Al_2O_3-P_2O_5$ glassforming system has so far been poorly developed and not well understood. Both Montagne et al.[6] and Lima et al.[7] reported the formation of opaque gels within a few minutes of mixing aluminum nitrate with sodium polyphosphate solution. Although the transparent xerogel was obtained through a gel-washing and centrifuging process, the final composition of such products is rather hard to control. Furthermore, these authors were unable to obtain glasses with this procedure. Processing of precursors is indeed known to influence greatly the formation, structure, and properties of sol−gel derived materials.[16] In this paper we present a novel Al-precursor, aluminum lactate, which has been used for the first time in the preparation of homogeneous transparent sodium aluminophosphate gels and glasses. We have also developed a procedure for the formation of transparent films on silica substrates and characterized these films by atomic force microscopy (AFM) and secondary neutral mass spectrometry (SNMS). To help optimize the preparation conditions for homogeneous gels it is highly desirable to gain mechanistic insights into the chemical reactions on a molecular level. To this end, previous studies have demonstrated the tremendous utility of ^{29}Si liquid- and solid-state NMR spectroscopy to monitor the various hydrolysis and condensation steps[17,18] as well as the gel-to-glass conversion of numerous siliceous systems.[19−22] In contrast, corresponding NMR studies of aluminophosphate systems have been relatively scarce. In the present contribution, we report detailed liquid- and solid-state NMR experiments to reveal the relevant species present in the precursor solutions to sodium aluminophosphate sols and gels and to monitor their conversion all the way to the solid glassy materials.

Experimental Section

Materials and Methods. Sodium aluminophosphate samples having the composition 43.8:12.5:43.8 $Na_2O/Al_2O_3/P_2O_5$ were prepared using sol−gel chemistry based upon the reaction of aluminum lactate with sodium polyphosphate ($NaPO_3$) in aqueous solutions. This particular composition was chosen because it corresponds to a level of aluminum incorporation above which dramatic changes are observed both in the bulk properties and the structural characteristics of melt-cooled glasses along the $NaPO_3-Al_2O_3$ compositional join.[23] Optimized synthesis procedures were developed based on aqueous solutions of the following reagents: $NaPO_3$ (95−97%, Fluka), aluminum lactate (98%, Fluka), HCl (1 M, puriss. p.a., Fluka), HNO_3 (1 M, puriss. p.a., Fluka), and NH_3 (1 M, diluted from concentrated ammonia solution, Aldrich). The pH of these solutions was adjusted with freshly prepared solutions of nitric acid or ammonia and controlled within 0.01 units by monitoring with a pH meter (WTW pH 320, Germany). Gel annealing was done in glass containers using a Heraeus muffle furnace. Crystallinity was checked via X-ray powder diffraction using the Guinier method, with Cu $K\alpha_1$ radiation and α-quartz (a = 491.30 pm, c = 540.46 pm) as an internal standard. Simultaneous differential thermal analysis and thermogravimetric analysis were carried out on a NETZSCH STA409 instrument using a heating rate of 10 K/min. Elemental compositions of film samples were characterized by the secondary neutral mass spectrometry (SNMS) technique using an INA 3 Leybold AG spectrometer operated in the high-frequency mode. Depth profiling of the films was carried out with krypton plasma sputtering. Atomic force microscopy (AFM) data were obtained with a Nanoscope 2 (Digital Instruments Inc., Santa Barbara, CA) under ambient conditions.

For comparison with the sol−gel materials, a bulk glass sample having the same composition (43.8:12.5:43.8 $Na_2O/Al_2O_3/P_2O_5$) was prepared by the melt cooling route. A stoichiometric mixture of $NaPO_3$ and Al_2O_3 (Fluka) was heated at 1350 °C for 3 h in a Pt crucible within a Nabertherm Supertherm furnace (HFL16/17). The sample was cooled rapidly to room temperature by removing the crucible from the furnace.

NMR Studies. Both the solution chemistry and the sol→gel→glass transformation were investigated by ^{27}Al and ^{31}P single and double resonance NMR techniques. These measurements were carried out at ambient temperature, at resonance frequencies of 130.3 and 202.5 MHz for ^{27}Al and ^{31}P, respectively, on a Bruker DSX-500 spectrometer, using a 4-mm MAS NMR probe. Liquid-state NMR studies were conducted on stationary samples located inside zirconia rotors, whereas solid-state NMR data were obtained at MAS rotation frequencies between 10 and 15 kHz. Typical 90° pulse lengths were 5.0 μs (^{31}P) and 3.0 μs (^{27}Al). The relaxation delays amounted to 60 and 1 s, for ^{31}P and ^{27}Al, respectively. Chemical shift referencing was done with external samples of a 1 M aqueous solution of $AlCl_3$ and 85% H_3PO_4. The ^{27}Al Hamiltonian parameters were measured with the triple-quantum (TQ)-MAS method using the three-pulse zero-filtering variant. To probe for $^{27}Al-^{31}P$ connectivities, the rotational echo double resonance (REDOR) technique was used. This approach uses special double irradiation methods to introduce the heteronuclear dipole−dipole interactions between the ^{27}Al and the ^{31}P nuclei − normally averaged out by MAS − back into the experiment. Specifically, the REDOR variant used in the present study records the rotor-synchronized ^{27}Al MAS NMR spin−echos while applying 180° pulses to the ^{31}P spins during the rotor period.[24] For qualitative measurements, the ^{27}Al signal intensities (S and S_o) obtained in the presence and the absence of ^{31}P irradiation were recorded. For more quantitative purposes whole REDOR curves $(S_o-S)/S_o$ were measured under systematic incrementation of the dipolar evolution time (NT_r = number of rotor cycles times rotor period). These

(10) Yoldas, B. E. *Am. Ceram. Soc. Bull.* **1975**, *54*, 289.
(11) McMahon, C. N.; Alemany, L.; Callender, R. L.; Bott, S. G.; Barron, R. A. *Chem. Mater.* **1993**, *11*, 181.
(12) Rezgui, S.; Gates, B. C. *J. Non-Cryst. Solids* **1997**, *210*, 287.
(13) Yudahara, S.; Takaya, I.; Chiba, J.; Kuroda, K. *J. Sol-Gel Sci. Technol.* **1997**, *8*, 95.
(14) Quartararo, J.; Guelton, M.; Rigole, M.; Amoureux, J. P.; Fernandez, C.; Grimblot, J. *J. Mater. Chem.* **1999**, *9*, 2637.
(15) Babonneau, F.; Coury, L.; Livage, J. *J. Non-Cryst. Solids* **1990**, *121*, 153.
(16) Szu, S. P.; Klein, L. C.; Greenblatt, M. *J. Non-Cryst. Solids* **1992**, *143*, 21. Szu, S. P.; Klein, L. C.; Greenblatt, M. *J. Non-Cryst. Solids* **1990**, *121*, 90.
(17) Kelts, L. W.; Effinger, N. J.; Melpolder, S. M. *J. Non-Cryst. Solids* **1986**, *83*, 353.
(18) Assink, R. A.; Kay, B. D. *J. Non-Cryst. Solids* **1988**, *99*, 359. Assink, R. A.; Kay, B. D. *J. Non-Cryst. Solids* **1988**, *107*, 35, and references therein.
(19) Yoldas, B. E. *J. Non-Cryst. Solids* **1986**, *83*, 375.
(20) Vega, A. J.; Scherer, G. W. *J. Non-Cryst. Solids* **1989**, *111*, 153.
(21) Wies, C.; Meise-Gresch, K.; Müller-Warmuth, W.; Beier, W.; Göktas, A. A.; Frischat, G. H. *Phys. Chem. Glasses* **1990**, *31*, 138.
(22) Wies, C.; Meise-Gresch, K.; Müller-Warmuth, W.; Beier, W.; Wellbrock, W.; Frischat, G. H. *J. Non-Cryst. Solids* **1990**, *116*, 161.
(23) Brow, R. K.; Kirkpatrick, R. J.; Turner, G. L. *J. Am. Ceram. Soc.* **1993**, *76*, 919.
(24) Gullion, T. S.; Schaefer, J. J. *Magn. Reson.* **1989**, *81*, 196.

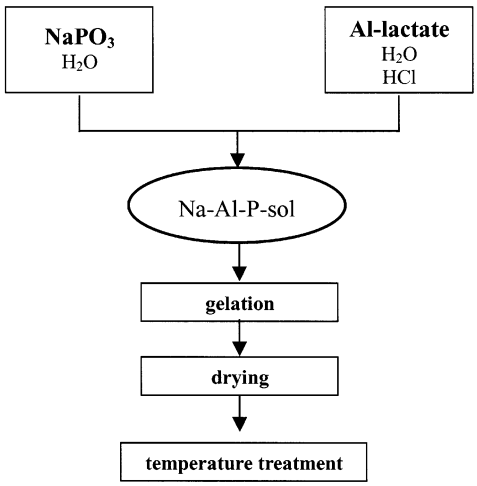

Figure 1. Flowchart depicting the sol−gel preparation route of sodium aluminophosphate glasses and thin films.

experiments were carried out at two different spinning speeds per data set, using 90° pulse lengths of 3 μs for both ^{27}Al (selective excitation conditions) and ^{31}P. The compensated REDOR method described in reference 25 was used for correcting the effects of small pulse imperfections. Using our previously established methodology[25,26] approximate dipolar second moments characterizing the magnitudes of these interactions were then obtained by detailed analysis of the REDOR curvatures in the limit of short dipolar evolution times ($0 \leq [(S_o - S)/S_o] \leq 0.2$).

Results and Discussion

Preparation and Properties of Bulk Samples. The following procedure was adopted for the preparation of bulk glassy materials (Figure 1). In a first step, sodium metaphosphate glass is obtained by cooling a melt of $NaPO_3$ from 700 °C to room temperature in a platinum crucible. Subsequently a 4 M solution (100 mL) was prepared by stirring 40.8 g of this glass in distilled H_2O for several hours in a glass container. In a typical preparation, 0.01 mol (∼3 g) of aluminum lactate was dissolved in 12 mL of distilled water, followed by the addition of 10 mL of sodium polyphosphate solution. The initial concentration of the sodium polyphosphate solution was adjusted to obtain the desired P/Al molar ratio in the mixture. The pH of these solutions was adjusted to the desired value (within 0.01 units) with freshly prepared solutions of nitric acid or ammonia. The resulting clear solution was gelled in the open atmosphere at 40−100 °C for several hours or at room temperature for several days. A monolithic transparent body was obtained initially, however, subsequent drying at elevated temperatures resulted in the formation of cracks (presumably because of the rapid liberation of volatiles). The sodium aluminophosphate glasses were obtained after heating the xerogels to 400 °C for several hours. Their noncrystalline state was confirmed by the absence of any sharp X-ray powder diffraction peaks. To eliminate entrapment of organics in the glass, the precursor gels needed drying under vacuum ($p < 10^{-4}$ mbar) at 150−200 °C for 8 h before they could be converted to glasses by further heat treatment. The latter conversion was done by increasing the temperature to 400 °C at a rate of 0.5 K per minute. Figure 2 summarizes the thermal analysis data. The thermogravimetric analysis (TGA) trace of the xerogel (Figure 2a) indicates that volatile components (organics and water) are almost completely driven off below 400 °C. In accordance with this result, sol−gel materials annealed at 400 °C show practically no weight loss due to incorporated organics (Figure 2b); the minor weight loss seen below 200 °C is most likely due to surface-adsorbed water in the sol−gel material. Finally, the glass transition and crystallization temperatures of the bulk glasses prepared by the sol−gel route and by the molten-state route are extremely similar (Figure 2c). The close structural similarity of both types of glasses is further confirmed by the solid-state NMR results, to be discussed in more detail below.

Preparation and Characterization of Thin Films. Films were prepared on pre-etched (1% HF for 30 s) silica substrates using the dip-coating process. In a typical run, substrates were dipped into a precursor solution made by mixing a solution (a) containing 1.785 g (0.0175 mol) of $NaPO_3$ in 20 mL of distilled water, with a second solution (b) containing 1.47 g (0.005 mol) of aluminum lactate and 1.25 g of 1 M HCl, and topped off with distilled water to 20 mL. In a second set of preparations the HCl was substituted by $HClO_4$ to facilitate oxidative removal of carbonaceous residues during the heating process. Films were heated at a rate of 6 K/min to 400 °C and kept at this temperature for durations of 1 and 4 h, respectively. Film properties were investigated with atomic force microscopy (AFM) and secondary neutral mass spectrometry (SNMS). Figure 3 shows typical AFM data illustrating that the acid (HCl or $HClO_4$) used for the film preparation has a considerable influence on the surface morphology. Whereas the material prepared with HCl has a relatively smooth surface with a roughness of ca. 0.2 nm, usage of $HClO_4$ produces an extremely uneven surface with a roughness in the 2−2.5 nm range. Comparison of Figure 3b and c indicates the roughness is also strongly influenced by the amount of $HClO_4$ used. The increased roughness may be attributed to the action of gaseous oxygen that is liberated during the heating process. Figure 4 shows SNMS depth-profiling data of a bulk glassy sample prepared by the melt-cooling route (a) and of films deposited on silica substrates (film thicknesses 50−90 nm, (b), (c), and (d)). Plotted are the signal intensities of the elemental constituents as a function of sputtering time. First of all, these data confirm that the elemental compositions achieved for the films are very similar to those of the bulk glass. Second, the data obtained for the film samples reflect − as expected − the transition from the sodium aluminophosphate layer to the silica substrate with increasing sputtering time. Finally, although the data do indicate the presence of residual carbon atoms in the films prepared from HCl-based solutions, they clearly show that the level of carbon contamination can be significantly reduced and even virtually eliminated when using sufficient amounts of $HClO_4$ in the deposition procedure (compare Figure 4b with c and d). This is important, as any residual carbon in the gel would significantly degrade the optical properties of the final

(25) Chan, J. C. C.; Eckert, H. J. *Magn. Reson.* **2000**, *147*, 170.
(26) Bertmer, M.; Eckert, H. *Solid State Nucl. Magn. Reson.* **1999**, *15*, 139.

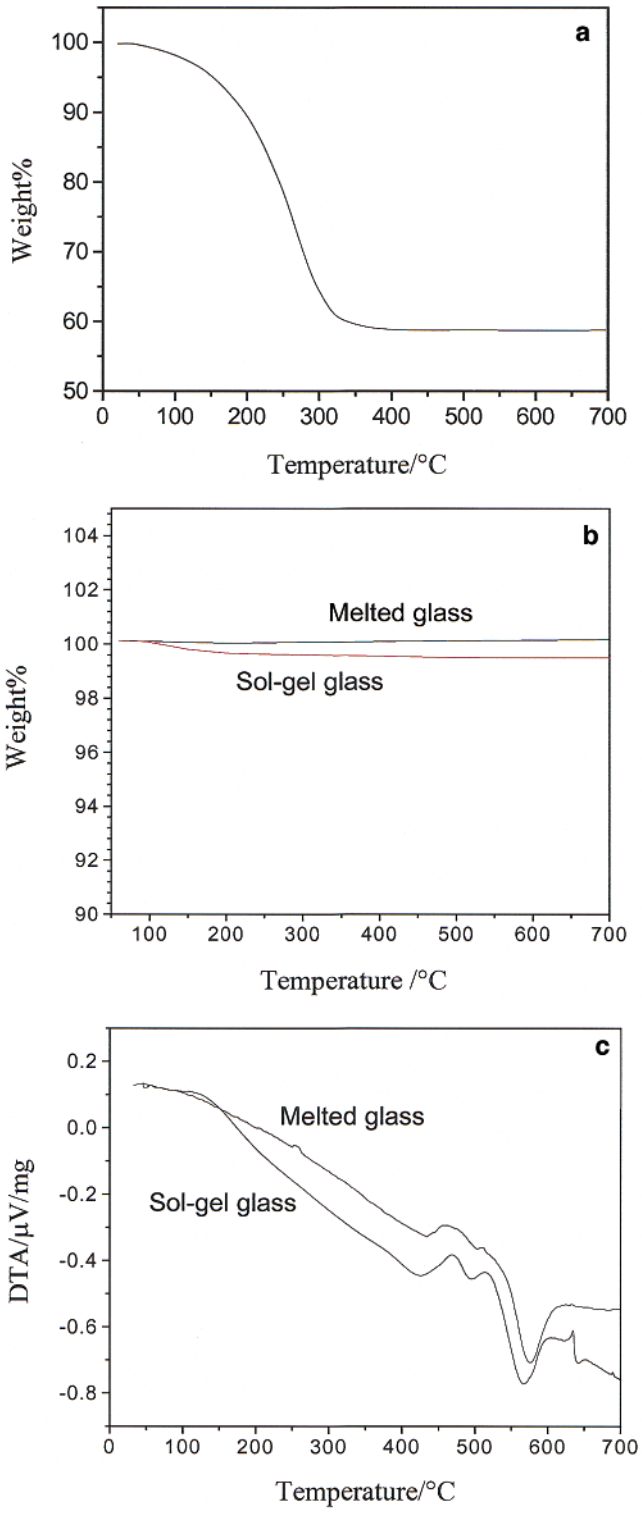

Figure 2. (a) TGA traces for the xerogel formed at room temperature, obtained at a heating rate of 10 K/min in air. Note that the weight loss of the xerogel is complete at 400 °C. (b) Thermogravimetric analysis of glass with composition 43.8%:12.5%:43.8% $Na_2O/Al_2O_3/P_2O_5$ prepared by the sol−gel route and by the traditional melt cooling method. The small weight losses observed in the TGA trace of sol−gel derived glass can be attributed to surface adsorbed water. (c) Differential thermal analysis of glass with composition 43.8%:12.5%:43.8% $Na_2O/Al_2O_3/P_2O_5$ prepared by the sol−gel route and by the traditional melt cooling method. The glass transition temperatures (onset points) observed in the DTA traces are 420 ± 10 °C and 440 ± 10 °C, respectively. The peaks near 570 °C denote recrystallization exotherms.

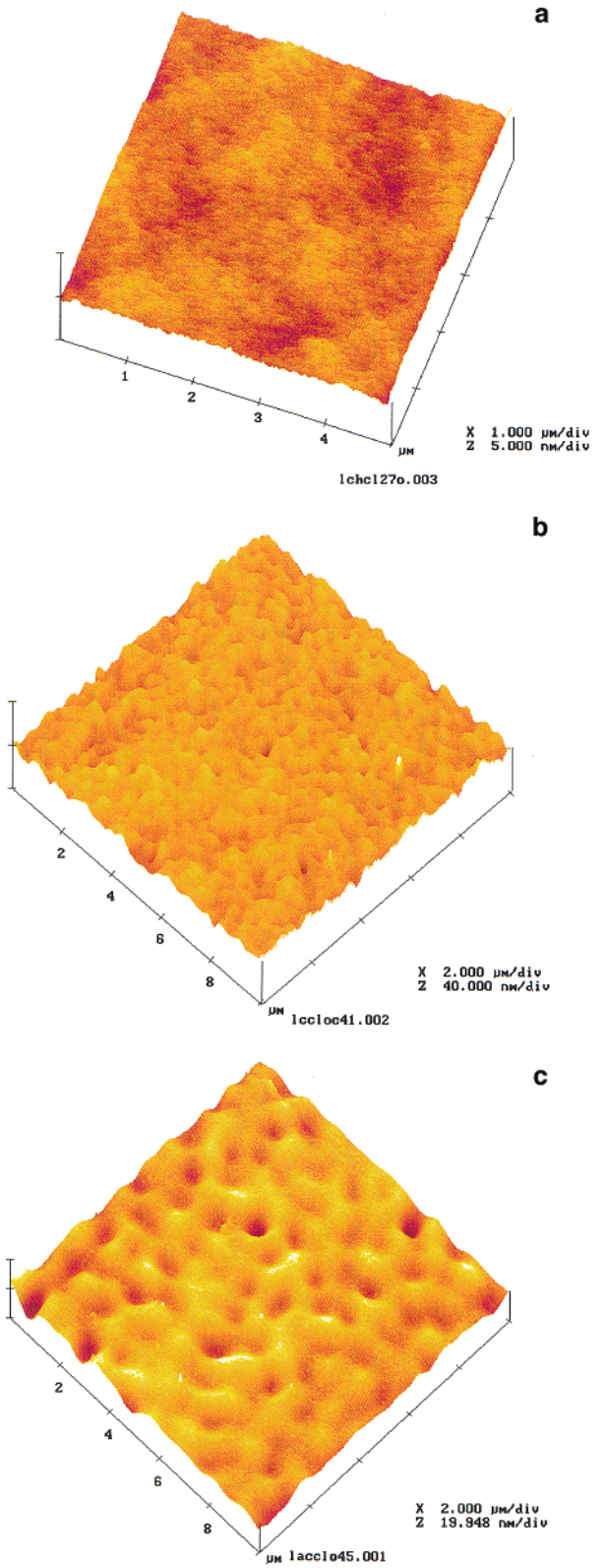

Figure 3. AFM surface characterization of 43.8%:12.5%:43.8% $Na_2O/Al_2O_3/P_2O_5$ thin films prepared under different conditions: (a) 1.25 mL of 1 M HCl as the acid component, annealed at 400 °C for 1 h; (b) 1.25 mL of 1 M $HClO_4$ as the acid component, annealed at 400 °C for 1 h; and (c) 5 mL of 1 M $HClO_4$ as the acid component, annealed at 400 °C for 1 h.

glassy materials obtained. Overall, the procedures developed in the present study permit the preparation of homogeneous and clear, transparent glassy sodium aluminophosphate thin films.

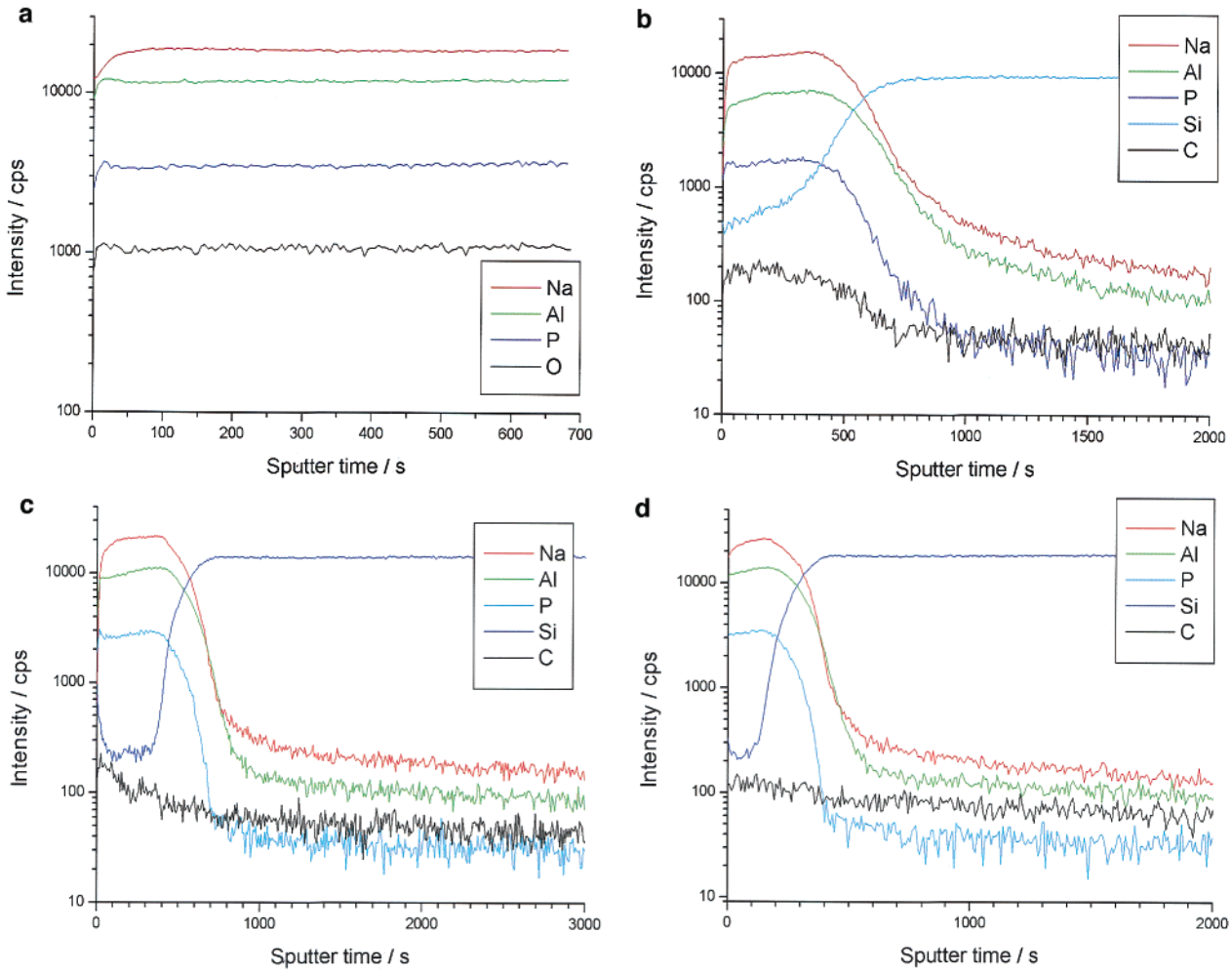

Figure 4. Secondary neutral mass spectrometry (SNMS) of sodium aluminophosphate glasses and thin films (on silica substrates) prepared under different conditions: (a) glass prepared by the melt-quenching route; (b) thin film, 1.25 mL of HCl as the acid component, annealed at 400 °C for 1 h; (c) thin film, 1.25 mL of 1 M $HClO_4$ as the acid component, annealed at 400 °C for 1 h; and (d) thin film, 5 mL of 1 M $HClO_4$ as the acid component, annealed at 400 °C for 1 h.

^{27}Al NMR Spectra of Precursor Solutions and Sols. To gain insight into the solution→ gel→ glass transition, ^{27}Al NMR experiments were recorded at the various processing steps. The spectra of the initial Al(lact)$_3$ aqueous solution are shown in Figure 5, as a function of pH. One can clearly differentiate four distinct species with chemical shifts around 0, 7.5, 14, and 22 ppm. At a low pH, e.g. pH ≤ 1.3, the dominant species observed at 0 ppm is $Al(H_2O)_6^{3+}$. At this pH, addition of sodium polyphosphate solution leads to the immediate formation of gels, which are, however, not transparent. As the pH of the precursor solution is raised, the signal contributions at 7.5, 14, and 22 ppm are seen to increase. On the basis of analogous studies conducted on aluminum glycolate[27] and tartrate[28] complexes, we can assign the signals at 7.5 and 14 ppm to $Al(lact)_1(H_2O)_4^{2+}$ and $Al(lact)_2(H_2O)_2^{+}$ species, respectively. It is in this pH range that we have observed the formation of clear transparent gels upon sodium polyphosphate addition. At even larger pH, e.g. pH = 4.7, the resonance at 22 ppm reflects the major species in solution. We assign this peak to the Al(lact)$_3$ complex, on the basis of previous ^{27}Al triple-quantum (TQ) MAS NMR data on crystalline Al(lact)$_3$ which reveal an isotropic chemi-

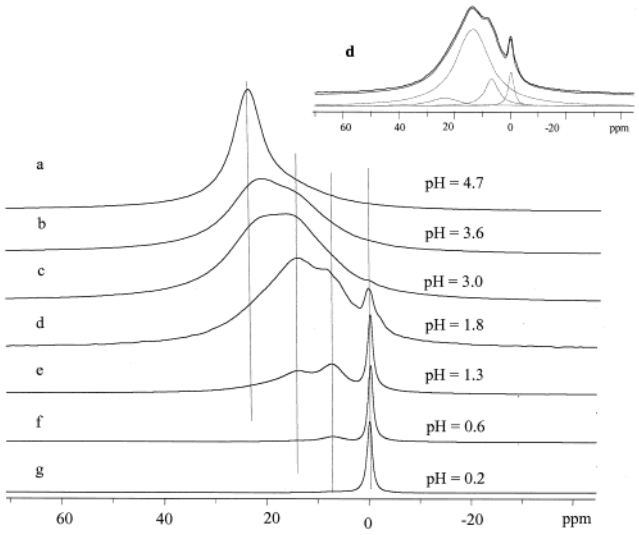

Figure 5. 130.2 MHz solution-state ^{27}Al NMR spectra of 0.5 M aluminum lactate solution as a function of pH value. The chemical shift regions of the different complexes are indicated by vertical lines. A typical spectral deconvolution for trace (d) is shown at the top.

(27) Venema, F. R.; Peters, J. A.; van Bekkum, H. *J. Chem. Soc., Dalton Trans.* **1990**, 2137.
(28) Venema, F. R.; Peters, J. A.; van Bekkum, H. *Inorg. Chim. Acta* **1992**, *191*, 261.

cal shift of 21.9 ppm.[29] The crystal structure of this compound shows Al in a distorted six-coordinated environment, where the lactate ligands are coordinated via both the carboxylate and the hydroxyl donating sites.[30]

On the basis of our solution-state NMR data, the hydrolysis process of aluminum lactate can be described schematically by eq 1. When increasing the concentration of H^+, the chemical equilibria will shift from $Al(lact)_3$ toward species with successively fewer lactate ligands.

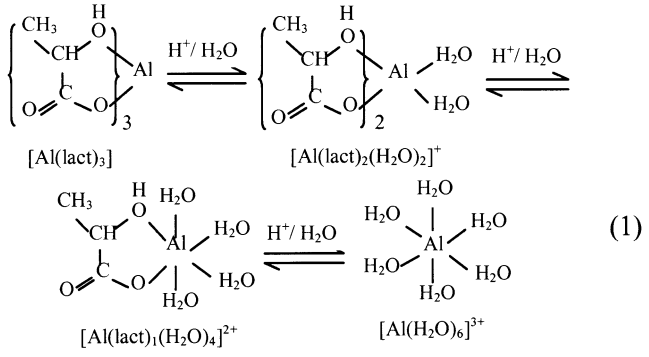

(1)

As Figure 5 illustrates, each of these complexes possesses a distinct NMR signature, although when spectra of samples at different pH levels are compared, somewhat variable line widths are observed for each species. This variability may reflect viscosity changes as a function of pH as well as chemical exchange phenomena occurring in the vicinity of the NMR time scale. Nevertheless, the resonances belonging to the mixed $Al(lact)_1(H_2O)_4^{2+}$ and the $Al(lact)_2(H_2O)_2^{+}$ species in general tend to be broader than those of the trilactate and the hexaquo complexes. This extra broadening can be attributed to more rapid quadrupolar relaxation caused by the larger fluctuating electric field gradients generated by these more asymmetric environments.

Addition of $NaPO_3$ solution to the Al−lactate solution leads to the production of clear sols and gels within the pH range $1.8 < pH < 3.6$. Figure 6 summarizes the ^{27}Al solution-state NMR spectra obtained after addition of 3.5 equivalents of $NaPO_3$, again as a function of pH (remeasured after addition). Although there is severe peak overlap, the spectra obtained for the various samples can be roughly divided into four chemical shift regions, as marked in the figure: a band (I) near 23 ppm, band (II) near 12 ppm, a band (III) near 3 ppm, and a band (IV) ranging from −5 to −10 ppm. Clearly, the peak near 23 ppm reflects the $Al(lact)_3$ species. As the pH is decreased the lactate ligand in the Al coordination sphere is now successively replaced by a mix of H_2O and PO_3^- ligands, producing increased shielding at the ^{27}Al nuclear sites. On the basis of results obtained on the phosphate free solutions (discussed above) we can assign the bands (II) and (III) at 12 and 3 ppm to the complexes with two and one lactate ligands, i.e., to $Al(lact)_2(H_2O)_{2-y}(PO_3)_y^{(1-y)+}$ $(0 < y < 2)$, $Al(lact)_1(H_2O)_{4-y}(PO_3)_y^{(2-y)+}$ $(0 < y < 4)$, respectively. As the broad spectra suggest, these resonances are affected

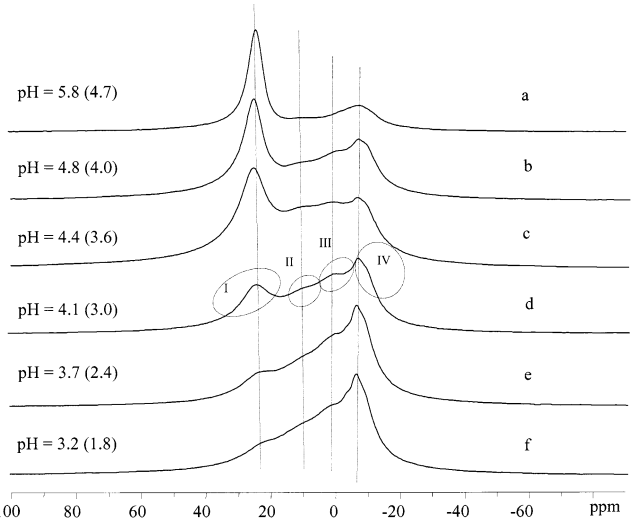

Figure 6. 130.2 MHz solution-state ^{27}Al NMR spectra of sols prepared by addition of a $NaPO_3$ glass solution to aluminum lactate solution as a function of pH value measured after the addition. (Values in parentheses give the pH values prior to addition of the $NaPO_3$ solution). The Al concentration of the resulting solution is 0.4 M. The chemical shift regions of species I−IV are indicated by vertical lines.

by rapid quadrupolar relaxation, making impossible the distinction of separate peaks attributable to species with discrete values of y, and enabling only the measurement of average chemical shifts. Band (IV) can be assigned to $Al(H_2O)_{6-y}(PO_3)_y^{(3-y)+}$ $(0 < y < 6)$ species, and for this component some partial resolution is visible in the spectrum, revealing the coexistence of various species corresponding to different y values. Replacement of a water molecule by a phosphate ligand (i.e., an increase in y) shifts the signal to lower resonance frequency. Figure 6 illustrates that − in analogy to the situation in the phosphate-free solutions (Figure 5) − the chemical species bearing fewer lactate ligands are successively favored as pH is decreased. Thus, the equilibria encountered in the phosphate-bearing solutions are best expressed by the following equation:

$$Al(lact)_3 + 2xH_2O \overset{H^+}{\leftrightarrow} Al(lact)_{3-x}(H_2O)_{2x}^{x+} + yPO_3^- \leftrightarrow Al(lact)_{3-x}(H_2O)_{2x-y}(PO_3)_y^{(x-y)+} \quad (2)$$

It is certain that the various species postulated in this scheme only start out mononuclear and subsequently polymerize to form polynuclear species. Thus, the formulae of eq 2 are to be understood as schematic depictions of the local aluminum environments only. The ^{27}Al solution-state NMR results of Figure 5 clearly indicate that the fractions of the mixed Al−lactate/hydro complexes $Al(lact)_1(H_2O)_4^{2+}$ and $Al(lact)_2(H_2O)_2^{+}$ are maximized in the pH range 1.8 to 3.6, where the optimum conditions for the formation of homogeneous sols and gels are found. It is likely that, owing to their molecular asymmetry, these mixed species are more reactive toward the phosphate substitution than the trilactate complex. This might explain the sensitive role of pH in controlling the gelation conditions in the aluminum lactate/sodium phosphate system.

^{27}Al NMR Characterization of the Gels and the Gel→ Glass Transition. Figure 7 shows the solid-state ^{27}Al NMR spectra of some xerogels formed at

(29) Van Wüllen, L.; Kalwei, M. *J. Magn. Reson.* **1999**, *139*, 250.
(30) Bombi, G. G.; Corain, B.; Sheikh-Osman, A. A. *Inorg. Chim. Acta* **1990**, *171*, 79.

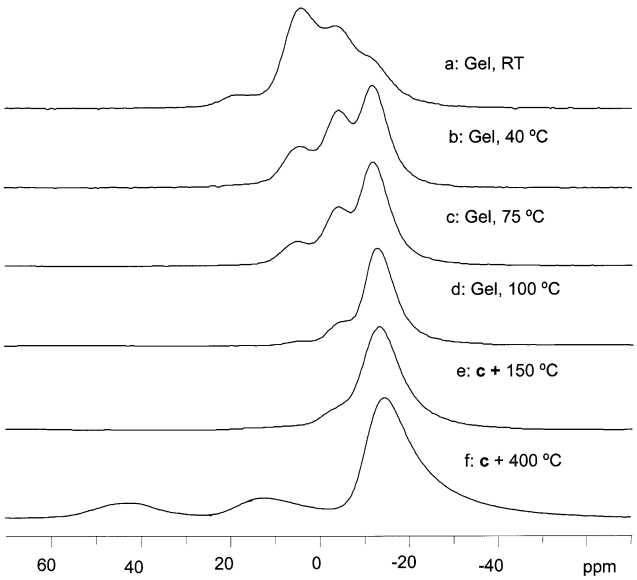

Figure 7. 130.2 MHz solid-state ^{27}Al NMR spectra of gels with composition 43.8%:12.5%:43.8% $Na_2O/Al_2O_3/P_2O_5$ showing the effect of gelation temperature and postsynthesis heating on the aluminum speciation.

different temperatures from the precursor solutions at pH 3.8. Four signal components are evident, with peak maxima near 22, 10, 0, and −10 ppm. The 22-ppm component can be readily assigned to $[Al(lact)_3]$. For the other signals, it appears reasonable to invoke the formation of mixed Al−lactate/phosphate species, namely $[Al(lact)_2(PO_3)_2]^-$ (at 10 ± 2 ppm), $[Al(lact)(PO_3)_4]^{2-}$ (at 0 ± 2 ppm), and $[Al(PO_3)_6]^{3-}$ (at −10 ± 2 ppm), respectively. These assignments were independently confirmed by ^{27}Al{^{31}P} REDOR experiments, which are sensitive to the number of P neighbors in the vicinity of each aluminum site.[31] Figure 7 illustrates that the average degree of Al/P connectivity in the xerogels can be controlled by the gel-processing temperature: as the latter is increased above room temperature, the equilibria in eq 2 are shifted toward the right. As a result, the $[Al(lact)_3]$ species is increasingly suppressed and the $[Al(PO_3)_6]^{3-}$ species is increasingly favored as the gel-processing temperature is raised from room temperature (RT, 25 °C) to 100 °C. Thus, increasing the gelation temperature above ambient favors the formation of inorganic materials free from organic residues. Postsynthesis heating of the xerogel to 150 °C results in further lactate ligand removal, as illustrated by Figure 7e, showing $[Al(PO_3)_6]^{3-}$ as the overwhelmingly dominant species.

After heating the gel sample at 400 °C for 4−8 h, the ^{27}Al solid-state NMR spectra show two new peaks near 45 and 13 ppm (Figure 7f). These peaks are also well-known in melt-cooled sodium aluminophosphate glasses, and have been assigned to $[Al(OP_4)]$ and $[Al(OP_5)]$ sites, respectively.[32−34] The ^{31}P NMR spectra can be deconvoluted into two separate contributions near −8 and −15 ppm. In conjunction with literature data,[33,34] these resonances are most probably assignable to pyrophosphate ($Q^{(1)}$) species having one and two aluminum neighbors (i.e., $Q^{(1)}_1$ and $Q^{(1)}_2$ species using the nomenclature of ref 33). Both the ^{27}Al and the ^{31}P MAS NMR spectra are virtually identical to those obtained on a sample prepared by conventional melt-cooling (Figure 8a). Figure 8b illustrates further that the ^{27}Al{^{31}P} REDOR results on both types of samples are essentially the same, revealing intimate Al−O−P connectivity for all the distinct Al(IV), Al(V), and Al(VI) coordination environments. This result confirms previous qualitative P/Al connectivity studies using related double resonance techniques.[33−35] We have analyzed the REDOR curvatures at short dipolar evolution times[26] in terms of site-selective ^{27}Al−^{31}P dipolar second moment values M_2^{Al-P}, best fit values of which are summarized in Table 1. Our results on the melt-cooled glasses are in good agreement with our earlier measurements.[35] For the AlO_6 and the AlO_4 sites the values are quite consistent with those measured in the crystalline model compounds $Al(PO_3)_3$ and $AlPO_4$, respectively,[25] the crystal structures of which maximize the degree of Al−O−P connectivity. On the basis of these results, we can conclude that in the sodium aluminophosphate glasses of the present study, the local environment of the Al atoms is also dominated by phosphorus. Most importantly, for each of the three aluminum environments present there are no significant differences in the degree of Al/P connectivity between the sol−gel prepared glasses and the melt-cooled glasses.

All of these results indicate convincingly that the local structures, the distributions of sites, and the degree of Al/P connectivity in the sol−gel derived glasses and those of the melt-cooled glasses are essentially indistinguishable. By all accounts both methods appear to lead to identical products. This is a remarkable result, in view of the fact that the maximum temperature used in the sol−gel process is only 400 °C, whereas the traditional glass-making technique requires melting temperatures of 1350 °C for the obtention of truly homogeneous and transparent samples.

Table 1. ^{27}Al Isotropic Chemical Shifts (δ_{cs}), Nuclear Electric Quadrupolar Coupling parameters P_Q[a], and ^{27}Al−^{31}P Dipolar Second Moments M_2^{Al-P} Measured for the Various Aluminum Species via TQMAS, and ^{27}Al{^{31}P} REDOR NMR Data for the Sol−Gel Prepared Glasses

sample	site	δ_{cs} (ppm)	P_Q[a] (MHz)	M_2^{Al-P} (KHz^2)
glass (sol−gel)	$Al(OP)_4$	51.0	3.8	5.3
$7Na_2O-2Al_2O_3-7P_2O_5$	$Al(OP)_5$	19.0	3.7	5.9
	$Al(OP)_6$	−10.3	2.9	6.2
glass (melt)	$Al(OP)_4$	50.8	3.7	5.1
$7Na_2O-2Al_2O_3-7P_2O_5$	$Al(OP)_5$	19.5	3.7	6.2
	$Al(OP)_6$	−10.2	3.0	6.4

[a] Nuclear electric quadrupolar coupling parameters P_Q is defined as $e^2qQ/h(1 + \eta^2/3)^{1/2}$.

Conclusions

In summary, we have developed a novel sol−gel route based on aluminum lactate aqueous solutions to prepare sodium aluminophosphate gels, glasses, and thin films. All of the macroscopic and spectroscopic characterization

(31) Zhang, L.; Eckert, H., to be published.
(32) Brow, R. K.; Kirkpatrick, R. J.; Turner, G. L. *J. Am. Ceram. Soc.* **1990**, *73*, 2293.
(33) Lang, D. P.; Alam, T. M.; Bencoe, D. N. *Chem. Mater.* **2001**, *13*, 420.
(34) Egan, J. M.; Wenslow, R. M.; Mueller, K. T. *J. Non-Cryst. Solids* **2000**, *261*, 115.
(35) Chan, J. C. C.; Eckert, H. *Phosphorus Res. Bull.* **1999**, *10*, 425.

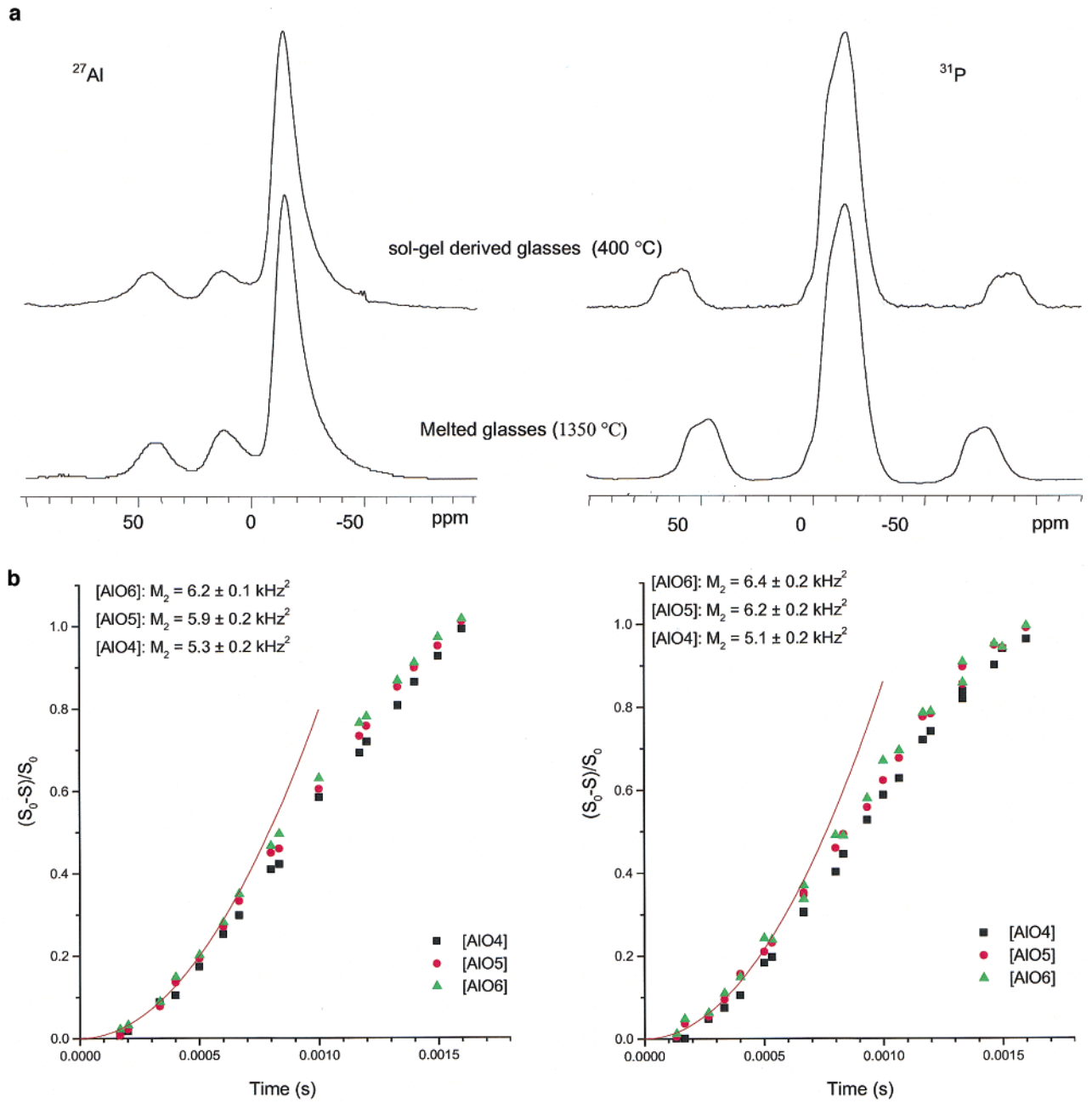

Figure 8. Spectroscopic comparison of the gel-prepared glasses with the melt-cooled glasses: (a) solid-state NMR spectra of ^{27}Al (left) and ^{31}P (right). In each of the spectra the top trace depicts the glasses prepared from the sol−gel route, and the bottom trace depicts the glasses prepared via melt-cooling from 1350 °C. (b) ^{27}Al{^{31}P}REDOR−NMR. Sol−gel prepared glasses are shown on left, and melt-cooled glasses are on the right. The different symbols denote the three different aluminum coordination environments for which site-resolved REDOR curves can be measured. The parabolic curves symbolize the fits for the ^{27}Al{^{31}P} REDOR data for the AlO_6 sites, yielding the M_2^{Al-P} values listed in Table 1. Similar fits (not shown) were obtained for the REDOR data on the AlO_5 and AlO_4 sites.

data indicate that the structures of the gel-route and the molten-state-route glasses are extremely closely related to each other. The excellent precursor properties of aluminum lactate are based on the fact that the degree of chelation, and hence the degree of reactivity, of the aluminum species can be controlled sensitively via the solution pH and temperature. On the basis of the solution and solid-state NMR data the optimum pH range for maximum homogeneity and Al/P connectivity found near pH 1.8−3.6 corresponds to the pH region in which the concentrations of the mixed $Al(lact)_1(H_2O)_4^{2+}$ and the $Al(lact)_2(H_2O)_2^{+}$ species are maximized. In addition, gelation temperatures above ambient favor the displacement of lactate by phosphate ligands, and residual lactic acid can be removed by vacuum annealing prior to the gel-glass conversion which is complete at temperatures near 400 °C. The carbon contents of the final glasses can be lowered even further if the precursor solutions contain $HClO_4$, as the gel heating process will then simultaneously result in oxidative removal of carbonaceous surface species. Work in our laboratory has shown that the sol−gel route developed here allows the preparation of homogeneous sodium aluminophosphate glasses with $NaPO_3/Al_2O_3$ ratios ranging from 1 to 9. This represents a not insignificant extension of the glass-forming range accessible by the melt-cooling method, as homogeneous glass with a P/Al molar ratio of unity is almost impossible to obtain by

traditional means.[36,37] Further preliminary studies have shown that aluminum lactate is also a good precursor candidate for numerous other sol−gel prepared alumina-based glasses and ceramics, such as the sodium aluminoborate system. The structural description of these materials will be the subject of a forthcoming publication.

(36) Brow, R. K. *J. Am. Ceram. Soc.* **1993**, *76*, 913.
(37) Kishioka, A.; Hayashi, M.; Kinoshita, M. *Bull. Chem. Soc. Jpn.* **1976**, *49*, 3032.

Acknowledgment. This work was funded by the Deutsche Forschungsgemeinschaft through grants Ec168/4-1 and Fr273/54-1 through the cooperative grant program "Vom Molekül zum Material". We are grateful to Ms. Wilma Pröbsting for the thermoanalytical characterization, to Ms. Zhiyun Wu for the XRD measurements, and to Mr. Thomas Peter for the SNMS measurements..

CM030155G